Atmos. Chem. Phys. Discuss., 9, 24511–24529, 2009
www.atmos-chem-phys-discuss.net/9/24511/2009/

Atmospheric Chemistry and Physics Discussions

This discussion paper is/has been under review for the journal Atmospheric Chemistry and Physics (ACP). Please refer to the corresponding final paper in ACP if available.

Relationship between wind speed and aerosol optical depth over remote ocean

H. Huang, G. E. Thomas, and R. G. Grainger

Atmospheric, Oceanic and Planetary Physics, University of Oxford, OX1 3PU, Oxford, UK

Received: 26 August 2009 – Accepted: 29 October 2009 – Published: 18 November 2009

Correspondence to: H. Huang (huang@atm.ox.ac.uk)

Published by Copernicus Publications on behalf of the European Geosciences Union.

Abstract

The effect of wind speed on aerosol optical depth (AOD) at 550 nm over remote ocean regions is investigated. Remote ocean regions are defined by the combination of AOD from satellite observation and wind direction from ECMWF. According to our definition, many oceanic regions cannot be taken as remote ocean regions due to long-range transportation of aerosols from continents. Highly correlated linear relationships are found in remote ocean regions with a wind speed range of 4–20 ms^{-1}. The enhancement of AOD at high wind speed is explained as the increase of sea salt aerosol production.

1 Introduction

Marine aerosol constitutes one of the largest natural aerosol systems and plays an important role in the Earth's radiative budget. It comprises two distinct aerosol types: (I) primary sea salt aerosol, and (II) secondary sulphate aerosol. Many studies show that sea salt particles make a significant contribution to both submicron and supermicron maritime aerosol modes (O'Dowd et al., 2001; Fitzgerald, 1991; Gras and Ayers, 1983; Heintzenberg et al., 2003; Hoppel et al., 1990; Clarke et al., 2003). The major sources of sea salt aerosol are the bursting of bubbles formed primarily by breaking waves, and mechanical disruption of wave crests by the wind (Exton et al., 1985; O'Dowd and de Leeuw, 2007; Andreas, 1998). Marine aerosol influences the radiative budget both directly and indirectly. These particles are the main contributor to light scattering in the cloud-free atmosphere in those regions with marine atmosphere. They also participate in cloud processes, serving as the dominant cloud condensation nuclei (CCN) source over the remote ocean regions (Hegg, 1992; Latham and Smith, 1990; Lohmann and Feichter, 2005; Ghan et al., 1998; Satheesha and Moorthy, 2005). Therefore elucidating the background sea salt aerosol is important to understanding the atmospheric radiative budget.

The effect of wind on aerosol over the oceans has been studied, but has mostly focused on the aerosol concentration and size distribution. Definite correlation was found between surface wind speed and sea-salt aerosol concentration (O'Dowd and Smith, 1993; Nilsson et al., 2001; McDonald et al., 1982). The influence of wind speed on marine AOD, τ, in the atmosphere is a much more difficult problem (Platt and Patterson, 1986; Villevalde et al., 1994; Smirnov et al., 1995; Moorthy et al., 1997). The link between marine aerosol optical properties and wind speed is difficult to quantify because it can be masked by long range transport from land based sources. Thus oceanic regions far from continents with no or less influence of long range transport is important for studying such a relationship.

Smirnov et al. (2003) reported that AOD measured at Midway Island, located in north-eastern Pacific Ocean at 28.12° N and 177.22° W, has a weakly correlated linear relationship with 24-h average surface wind speed. Other studies have also reported similar relationships (Jennings et al., 2003; Smirnov et al., 1995; Villevalde et al., 1994). Moorthy and Satheesh (2000) found an exponential increase in daily averaged AOD with wind speed at the island of Minicoy in the Arabian Sea. However, the region in this study is close to land so that it cannot be considered as a pristine marine environment. Mulcahy et al. (2008) obtained a power-law relationship between wind speed and AOD at four different wavelengths at Mace Head, located on the west coast of Ireland. This site is similarly not representative of the remote ocean. Based on one month of τ data from the Sea-viewing Wide Field-of-view Sensor (SeaWiFS) and surface wind data from ECMWF, Glantz et al. (2009) found a power-law relationship between surface wind speed and AOD for the north Pacific. However in their study, a single surface reflectance value was used in the retrieval of AOD from SeaWiFS. The influence of whitecaps generated by enhanced wind speed could cause spurious backscatter and influence the retrieved aerosol loading.

Though many studies have been performed, there is still no consensus on the relationship between wind speed and observed AOD. Additionally, all of the previous studies were from different locations using different instruments and also in different time periods. Hence a direct comparison between their results is difficult to make and it is hard to extrapolate their results to other areas. Also, some locations where the experiments were carried out are close to continents. In this paper, we first determine which oceanic areas can be taken as remote ocean, based on the wind directions and AOD, and then we investigate the relationship between AOD and wind speed over these regions, where the influence of continental aerosols can be considered minimal. The paper is organized as follows: In Sect. 2, we briefly explain the data and the instruments used. A quantitative method to distinguish remote oceanic regions from areas influenced by continental outflow is introduced in Sect. 3. Preliminary results are presented in Sect. 4. Concluding remarks are given in Sect. 5

2 Data

Aerosol data used in this paper were the AOD at 550 nm, τ, retrieved from Advanced Along-Track Scanning Radiometer (AATSR) as part of the ESA GlobAEROSOL project (Thomas et al., 2008). AATSR is on board the European Space Agency's Envisat platform, which is in a sun-synchronous orbit with an overpass time of 10:30 a.m. local solar time. AATSR acquires two near-simultaneous observations of the same area of the Earth's surface at a viewing angle of 55° (forward view at the surface) and then approximately 90 s later at an angle close to vertical (nadir view). The dual-view allows AATSR to retrieve surface reflectance and τ independently, and the changes in surface reflectance do not influence the precision of the τ retrieval (Sayer, 2008). The data used in this paper have a resolution of 1°×1°, obtained daily for the whole year of 2004 over the global oceanic regions. The 10-m wind speed from ECMWF is used in this paper at the same spatial resolution as the τ data. The wind fields have been interpolated to Envisat nominal local overpass time. Based on zonal (u) and meridional (v) wind components given by ECMWF, the wind speed (s) is calculated using $s=\sqrt{u^2+v^2}$ and wind direction is defined as shown in Fig. 1.

3 Method

To get a clear understanding of the relationship between wind speed and τ, the first step is to define the remote ocean regions. A heuristic argument can be made that, for truly remote oceanic regions, the only aerosol source is the ocean and thus the τ should not depend on wind direction but only on wind speed and other parameters such as temperature and relative humidity. For each $1^{\circ}\times 1^{\circ}$ point in the global ocean, the daily τ data are sorted into different bins according to the corresponding wind direction. Figure 1b illustrates a simple example with only 8 bins chosen. In practice, thirty-six 10° bins are used. We then calculate the average value of τ in each bin and the standard deviation of the average value over all wind directions σ_τ. The value of σ_τ indicates the dependence of τ on wind direction. If σ_τ is large, τ at the this point changes markedly as wind direction changes, indicating that a possible external source of aerosol exists. On the other hand, if the σ_τ is small, τ shows no or weak dependence on wind direction, indicating that the corresponding area is a possible pristine oceanic candidate. This is shown stylistically in Fig. 2.

The histogram of σ_τ for all global oceanic points is plotted in Fig. 3.. The main peak in Fig. 3 is interpreted as the typical variability of τ as a function of direction. The large tail of high variability denotes aerosol being transported from preferred directions. To differentiate locations with typical τ, from those demonstrating a preferred direction we have used a threshold, $\sigma_\tau^{\mathrm{th}}$, of about 2/3 of the peak values (i.e. a value of 0.035). For any point, if $\sigma_\tau \geq \sigma_\tau^{\mathrm{th}}$, it implies there are possible external aerosol sources other than the ocean itself: we take this type of point to be non-remote ocean.

It is interesting to look at those points that are identified as being non-remote ocean. For these points, the corresponding angle $\theta_{\max}$ is found where the averaged τ is maximum. This $\theta_{\max}$ indicates a possible important direction of aerosol transport to the given region.

ACPD

9, 24511–24529, 2009

4 Results

A map of θ_{max} for the points where σ_τ is greater than σ_τ^{th} is shown in Fig. 4, indicating the source direction of transported aerosols for these points. This map roughly matches the large-scale flow field and storm tracks. For the mid-latitude ocean (30° N–60° N) Northern Hemisphere, enhanced aerosol loading occurs when the wind direction is westerly, taking heavy-industry pollutants from East Asia and North America.

For the tropical and sub-tropical Atlantic regions, it is obvious that North Africa is the main source of aerosol for surrounding areas. Over the sub-tropical and tropical Atlantic ocean, the σ_τ^{max} matches the direction of trade winds that transport dust from the Sahara. The largest value of τ occurs in the Persian Gulf, where wind comes from the south west. For the points located in the east central Pacific, τ is maximum with east wind, indicating that the large values of τ over these points probably relate to long range transport aerosol from biomass burning in South America or dust from the Sahara. Over the west central Pacific, as well as the southern China sea, τ is largest when wind comes from a roughly northerly direction. This could be related to sand storms in northern China and Mongolia.

Over the southern oceans (between 30° S–60° S), the largest τ occurs with wind directions in a range of 70° to 140° (see Fig. 1a), i.e. westerlies. As there are no large continents in this region, this zonal region could be thought of as a remote ocean region, with little influence from continents. From this map, many regions, especially in the Northern Hemisphere, cannot be regarded as pure remote oceans. This interpretation is supported by the carbon monoxide (CO) distribution map from Measurements Of Pollution In The Troposphere (MOPITT) (see Fig. 5). The two main sources for CO are industrial pollution and biomass burning (Singer, 1975; Sanderson, 2002). The high CO in the Northern Hemisphere indicates that those regions may be influenced by long distance transportation from land, while the regions between 30° S–60° S have relatively low CO concentrations. Experiments with a long time-period (more than one

ACPD

9, 24511–24529, 2009

Relationship between wind speed and AOD

H. Huang et al.

Title Page
Abstract | Introduction
Conclusions | References
Tables | Figures
◂ | ▸
Back | Close
Full Screen / Esc
Printer-friendly Version
Interactive Discussion

year) aimed at measuring aerosol properties over remote ocean could lead to unreliable results for such regions.

Based on this analysis, we have chosen remote ocean points over three regions, shown as black frames in Fig. 4. Since they suffer less influence from land, the loading aerosols for these regions are free from contamination by long-range transported aerosol, it is easy to detect the link between marine AOD, τ, and wind speed. The relationship between wind speed and τ for these regions is plotted in Figs. 6 to 8. All plots show a similar relationship between wind speed and τ, which is largely linear up to s=20 ms^{-1}. The AOD is observed to increase by around 0.1 over a wind speed range of 4 to 20 ms^{-1}. We interpret this significant increase to the enhanced contribution of sea-salt particles. Importantly, there is no indication that an exponential function is a better fit to the measurements than a straight line. A linear (green line) and an exponential curve (red line) are fitted to the data. Figure 9 shows the average relationship among the three regions. τ over the remote oceans increases with sea surface wind speed following a linear relation of the form:

$$\tau = a + b \times s \quad (1)$$

where a and b are constants. The gradient b has a value of 0.0040±0.0002 and the offset, a, has a value 0.0850±0.0002. Similar results are obtained based on annual data of 2003 where the value of a is 0.094 and that of b is 0.003. This result is different from Mulcahy et al. (2008) and Glantz et al. (2009), which are taken from the northern Pacific and northern Atlantic respectively, but is very similar to the results of Smirnov et al. (2003) and Jennings et al. (2003), which were taken from Midway Island and Tahiti, which are largely thought to be remote ocean areas due to their long distances from the mainland.

5 Conclusions

In this study, we have examined the oceanic τ at 550 nm obtained from AATSR as a function of the surface wind fields from the ECMWF. The remote ocean region is defined by its wind direction and τ. Using this criteria, the majority of the oceans cannot be considered pristine remote ocean, as they show evidence of aerosol transport from land airmasses. A linear relationship with high correlation coefficients is found between wind speed and τ at 550 nm in clear marine environments, suggesting an important sea-salt contribution to τ. This work extends such a relationship to wind speed of 20 ms^{-1}, higher than in previous studies. We show that under strong wind conditions the τ in clear marine atmosphere could be as high as 0.2. Our study indicates there is an important effect of wind speed on the total τ in remote oceans. The changing wind pattern caused by climate change could lead to significant changes in τ over oceans and could influence both direct and indirect (via interaction with clouds) aerosol radiative forcing, as well as chemical and biological processes in atmosphere.

Acknowledgements. Haiyan Huang acknowledges the support of a KC Wong award. This work was supported by the Natural Environment Research Council (grant number NE/E011187/1).

References

Andreas, E. L.: A New Sea Spray Generation Function for Wind Speeds up to 32 m s1, J. Phys. Oceanogr., 28, 2175–2184, 1998. 24512

Clarke, A., Kapustin, V., Howell, S., and Moore, K.: Sea-Salt Size Distributions from Breaking Waves: Implications for Marine Aerosol Production and Optical Extinction Measurements during SEAS, J. Atmos. Ocean. Tech., 20, 1362–1374, 2003. 24512

Exton, H. J., Latham, J., Park, P. M., Perry, S. J., Smith, M. H., and Allan, R. R.: The production and dispersion of marine aerosol, Q. J. Roy. Meteorol. Soc., 111, 817–837, 1985. 24512

Fitzgerald, J. W.: Marine aerosols: a review, Atmos. Environ., 25A, 533–546, 1991. 24512

Ghan, S. J., Guzman, G., and Abdul-Razzak, H.: Competition between Sea Salt and Sulfate Particles as Cloud Condensation, J. Atmos. Sci., 55, 3340–3347, 1998. 24512

Glantz, P., Nilsson, E. N., and Hoyningen-Huene, W.: Estimating a relationship between aerosol optical thickness and surface wind speed over the ocean, Atmos. Res., 92, 58–68, 2009. 24513, 24517
Gras, J. L. and Ayers, G. P.: Marine aerosol at southern mid-latitudes, J. Geophys. Res., 88, 10661–10666, 1983. 24512
Hegg, D. A.: Modelling the effects of heterogeneous cloud chemistry on the marine particle size distribution, J. Geophys. Res., 97, 12927–12933, 1992. 24512
Heintzenberg, J., Covent, D. C., and Dongenen, R. V.: Size distribution and chemical composition of marine aerosols: a compilation and review, Tellus B, 52, 1104–1122, 2003. 24512
Hoppel, W. A., Fitzgerald, J. W., and Mack, E. J.: Aerosol size distributions and optical properties found in the marine boundary layer over the Atlantic Ocean, J. Geophys. Res., 95, 3659–3686, 1990. 24512
Jennings, S. G., Kleefeld, C., O'Dowd, C. D., Junker, C., Spain, T. G., O'Brien, P., Roddy, A. F., and O'Connor, T. C.: Mace Head Atmospheric Research Station Characterization of aerosol radiative parameters, Boreal Environ. Res., 8, 303–314, 2003. 24513, 24517
Latham, J. and Smith, M. H.: Effect on global warming of wind-dependent aerosol generation at the ocean surface, Nature, 347, 372–373, 1990. 24512
Lohmann, U. and Feichter, J.: Global indirect aerosol effects: a review, Atmos. Chem. Phys., 5, 715–737, 2005, http://www.atmos-chem-phys.net/5/715/2005/. 24512
McDonald, R. L., Unni, C. K., and Duce, R. A.: Estimation of atmospheric sea salt dry deposition: Wind speed and particle size dependence, J. Geophys. Res., 87(C2), 1246–1250, 1982. 24513
Moorthy, K. K. and Satheesh, S. K.: Characteristics of aerosols over a remote island, Minicoy in the Arabian Sea: Optical properties and retrieved size characteristics, Q. J. Roy. Meteorol. Soc., 126, 81–109, 2000. 24513
Moorthy, K. K., Satheesh, S. K., and Murthy, B. V. K.: Investigations of marine aerosols over the tropical Indian Ocean, J. Geophys. Res., 102, 827–842, 1997. 24513
Mulcahy, J. P., O'Dowd, C. D., and Ceburnis, S. G. J. D.: Significant enhancement of aerosol optical depth in marine air under high wind conditions, Geophys. Res. Lett., 35, L16810–L16813, 2008. 24513, 24517
Nilsson, E. D., Rannik, U., and Norman, M.: Turbulent aerosol fluxes over the Arctic Ocean 2. Wind-driven sources from the sea, J. Geophys. Res., 106, 32139–32154, 2001. 24513

O'Dowd, C. D. and de Leeuw, G.: Marine aerosol production: a review of the current knowledge, Philos. T. Roy. Soc, 365, 1753–1774, 2007. 24512
O'Dowd, C. D. and Smith, M. H.: Physicochemical properties of aerosols over the northeast Atlantic: Evidence for wind-speed-related submicron sea-salt production, J. Geophys. Res., 98, 1137–1149, 1993. 24513
O'Dowd, C. D., Smith, M. H., Consterdine, I. E., and Lowe, J. A.: Marine aerosol, sea-salt, and the marine sulphur cycle: a short review, Atmos. Environ., 10, 1352–2310, 2001. 24512
Platt, C. M. R. and Patterson, G. R.: The interpretation of baseline atmospheric turbidity measurements at Cape Grim, Tasmania, J. Atmos. Chem., 4, 187–197, 1986. 24513
Sanderson, M. G.: Emission of carbon monoxide by vegetation and soils, Tech. rep., 1–3, 2002. 24516
Satheesha, S. K. and Moorthy, K. K.: Radiative effects of natural aerosols: A review, Atmos. Environ., 39, 2089–2110, 2005. 24512
Sayer, A.: Aerosol Remote Sensing Using AATSR, Ph.D. thesis, University of Oxford, 2008. 24514
Singer, S. F.: The Changing global environment, D. Reidel Publ. Co., Dordrecht-Holland/Boston-USA, 1975. 24516
Smirnov, A., Villevalde, Y., O'Neill, N. T., Royer, A., and Tarussov, A.: Aerosol optical depth over the oceans: Analysis in terms of synoptic air mass types, J. Geophys. Res., 16, 639–650, 1995. 24513
Smirnov, A., Holben, B. N., Dubovik, O., Frouin, R., Eck, T. F., and Slutsker, I.: Maritime component in aerosol optical models derived from Aerosol Robotic Network data, J. Geophys. Res., 108(D1), 1–100, 2003. 24513, 24517
Thomas, G. E., Carboni, E., Poulsen, C., Siddans, R., Grainger, D., Kerridge, B., and Gomez, C.: GlobAerosol: A 12 year global aerosol dataset from European satellite instruments, 2nd MERIS/(A)ATSR User Workshop, 2008. 24514
Villevalde, Y. V., Smirnov, A. V., O'Neill, N. T., Smyshlyaev, S. P., and Yakovlev, V. V.: Measurement of aerosol optical depth in the Pacific Ocean and the North Atlantic, J. Geophys. Res., 99, 983–988, 1994. 24513

ACPD
9, 24511–24529, 2009

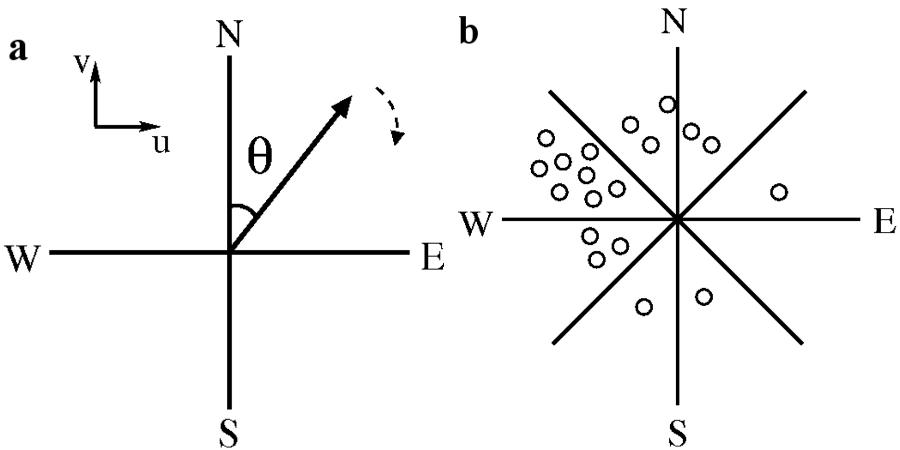

Fig. 1. (a) Definition of wind direction. **(b)** τ daily data (indicated by the circles) are categorised by wind direction.

ACPD
9, 24511–24529, 2009

Relationship between wind speed and AOD

H. Huang et al.

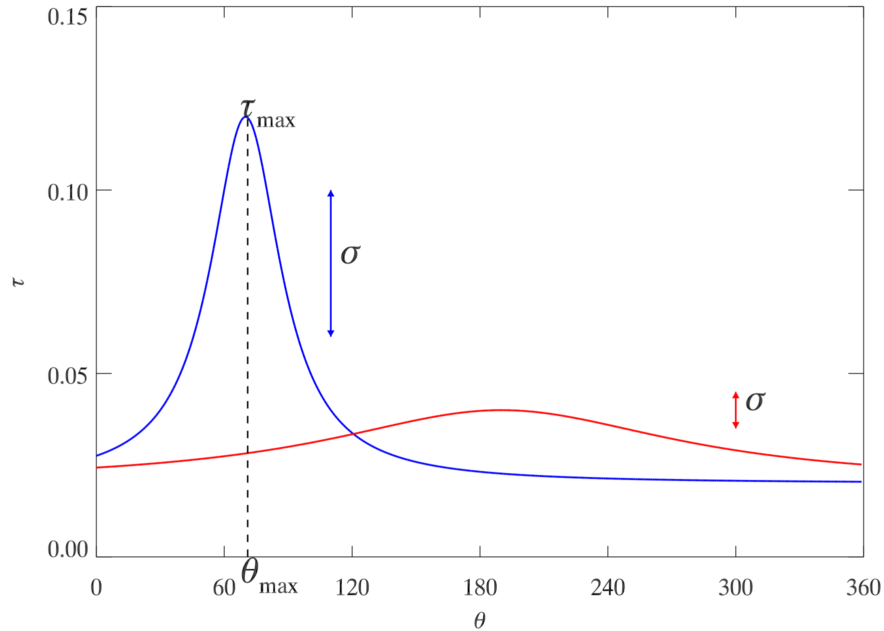

Fig. 2. For each 1°×1° point, τ is expressed as a function of wind direction. The blue curve represents the case where τ depends strongly on wind direction and so has a large σ_τ. The red curve represents the case where τ does not depend on wind direction and so has a small σ_τ.

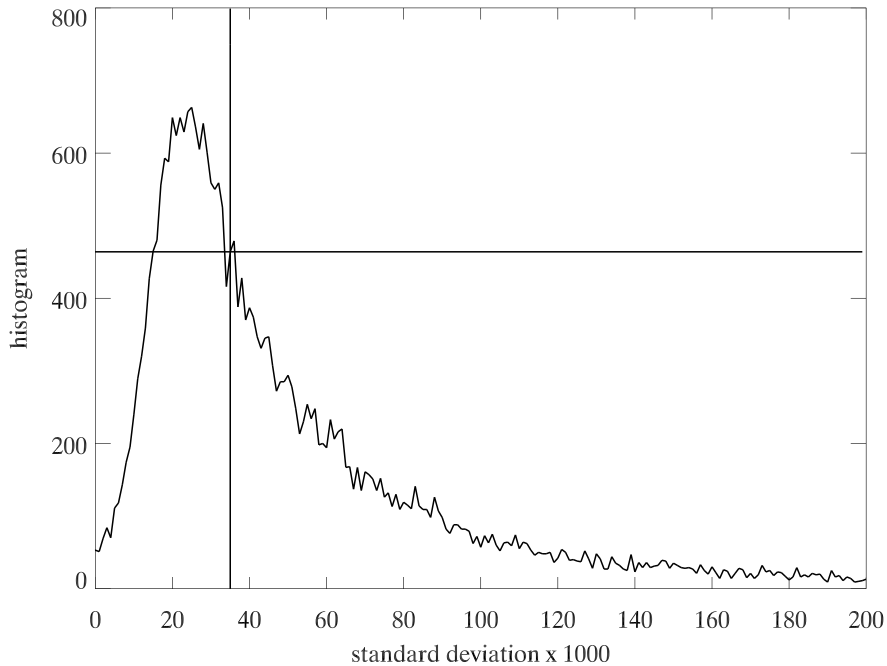

Fig. 3. Histogram of σ_τ for global ocean points.

ACPD
9, 24511–24529, 2009

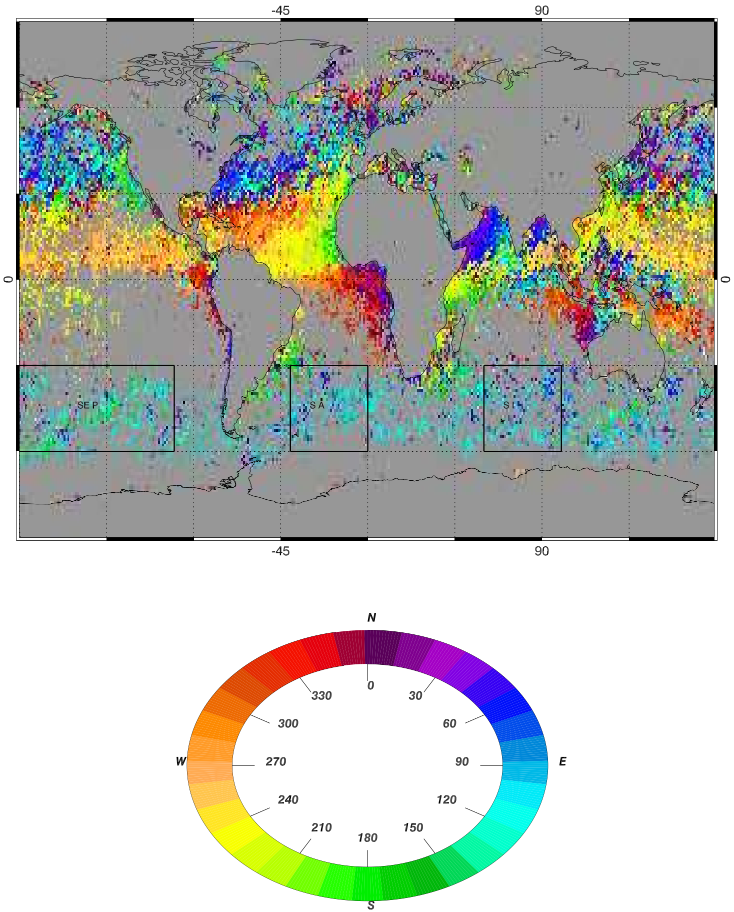

Fig. 4. Plot of wind direction θ_{max} for the locations where σ_τ is greater than 0.035. Rectangular frames show regions discussed.

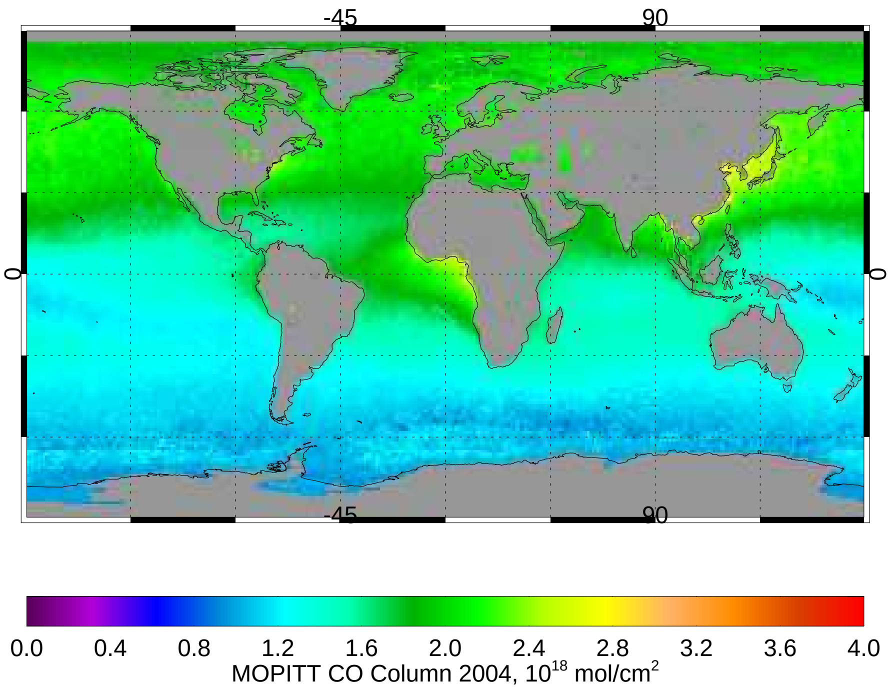

Fig. 5. Column CO distribution from MOPITT, 2004.

ACPD
9, 24511–24529, 2009

Relationship between wind speed and AOD

H. Huang et al.

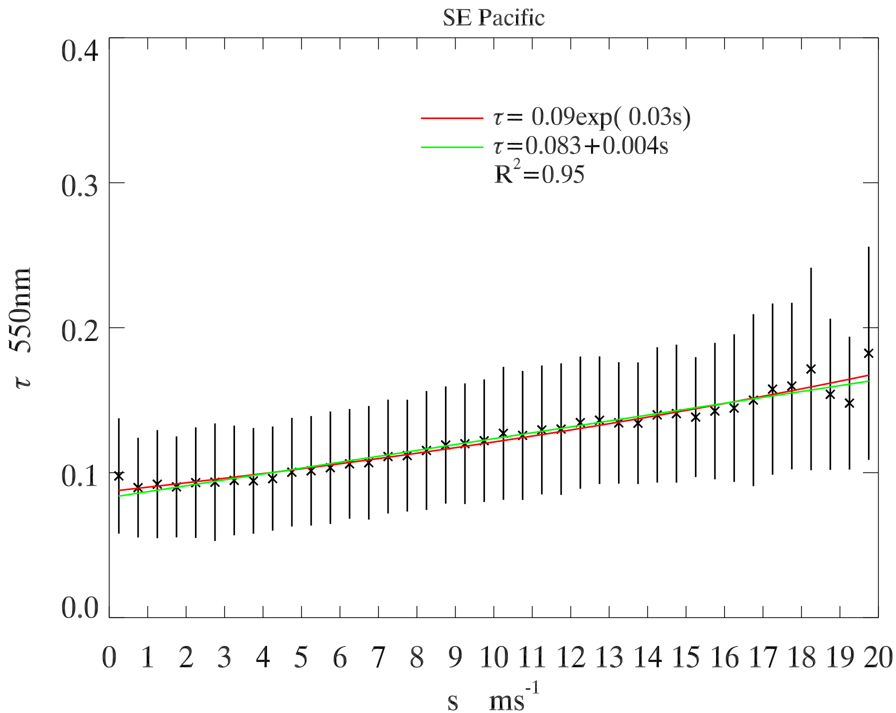

Fig. 6. Relationship between wind speed and τ over the South East Pacific ocean region.

ACPD
9, 24511–24529, 2009

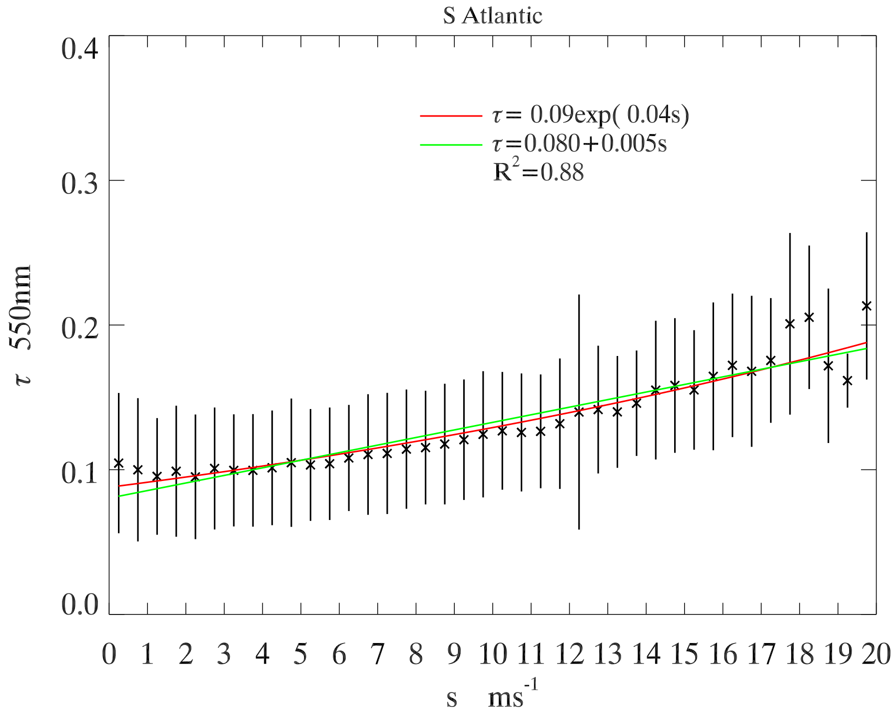

Fig. 7. Relationship between wind speed and τ over the South Atlantic ocean region.

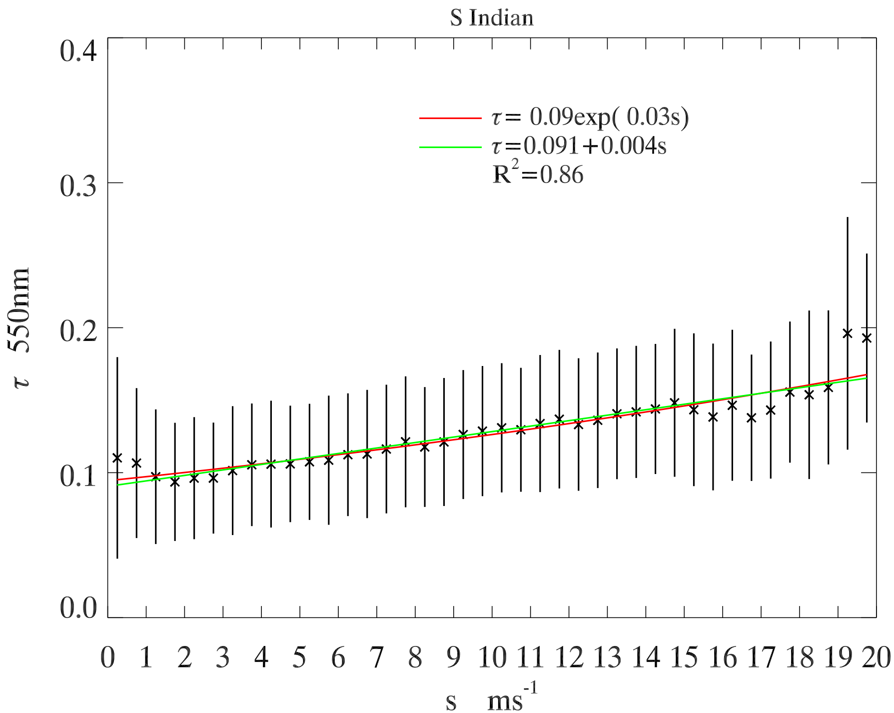

Fig. 8. Relationship between wind speed and τ over South Indian ocean region.

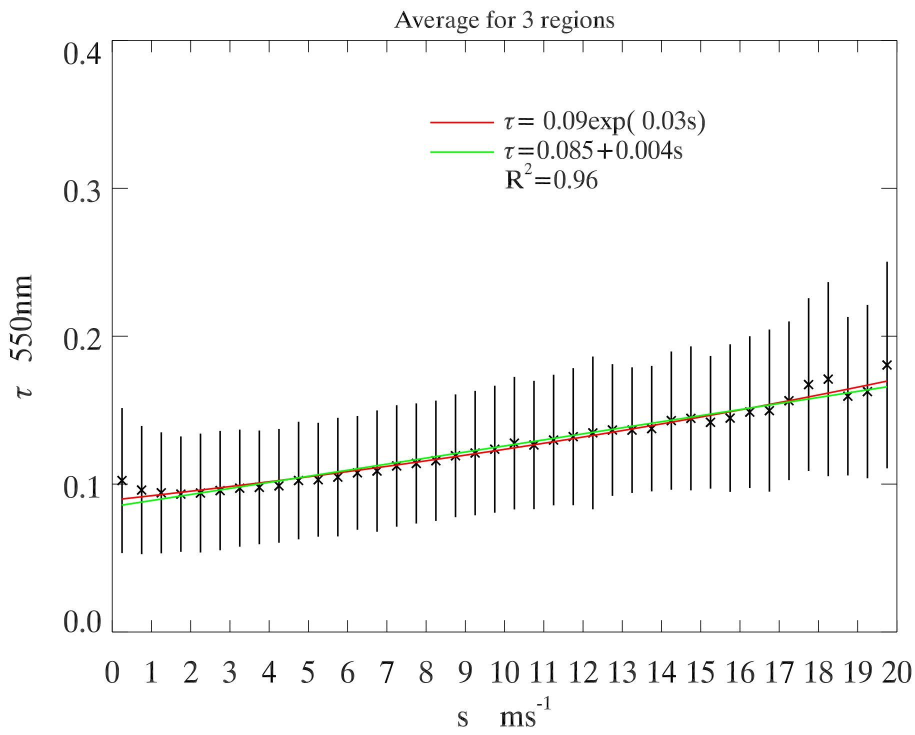

Fig. 9. Relationship between wind speed and τ over the three regions.

ACPD
9, 24511–24529, 2009

Relationship between wind speed and AOD

H. Huang et al.